

MIT Open Access Articles

Authenticated storage using small trusted hardware

The MIT Faculty has made this article openly available. **Please share** how this access benefits you. Your story matters.

Citation: Hsin-Jung Yang, Victor Costan, Nickolai Zeldovich, and Srinivas Devadas. 2013. Authenticated storage using small trusted hardware. In Proceedings of the 2013 ACM workshop on Cloud computing security workshop (CCSW '13). ACM, New York, NY, USA, 35-46.

As Published: <http://dx.doi.org/10.1145/2517488.2517494>

Publisher: Association for Computing Machinery (ACM)

Persistent URL: <http://hdl.handle.net/1721.1/86161>

Version: Author's final manuscript: final author's manuscript post peer review, without publisher's formatting or copy editing

Terms of use: Creative Commons Attribution-Noncommercial-Share Alike



Authenticated Storage Using Small Trusted Hardware

Hsin-Jung Yang, Victor Costan, Nikolai Zeldovich, and Srinivas Devadas
Computer Science and Artificial Intelligence Laboratory
Massachusetts Institute of Technology
Cambridge, Massachusetts, United States
{hjiang, costan, nickolai, devadas}@mit.edu

ABSTRACT

A major security concern with outsourcing data storage to third-party providers is authenticating the integrity and freshness of data. State-of-the-art software-based approaches require clients to maintain state and cannot immediately detect forking attacks, while approaches that introduce limited trusted hardware (e.g., a monotonic counter) at the storage server achieve low throughput. This paper proposes a new design for authenticating data storage using a small piece of high-performance trusted hardware attached to an untrusted server. The proposed design achieves significantly higher throughput than previous designs. The server-side trusted hardware allows clients to authenticate data integrity and freshness without keeping any mutable client-side state. Our design achieves high performance by parallelizing server-side authentication operations and permitting the untrusted server to maintain caches and schedule disk writes, while enforcing precise crash recovery and write access control.

Categories and Subject Descriptors

D.4.6 [Security and Protection]: Authentication

Keywords

Secure storage; Trusted hardware; Authentication; Integrity; Freshness; Replay attack; Forking attack

1. INTRODUCTION

Cloud-based data storage services are becoming increasingly popular, allowing users to back up their data remotely, access the data from any connected device, as well as collaborate on the shared data. For example, Amazon S3 [1] and Google Storage [17] offer scalable storage services to end users, enterprises, and other cloud services providers. Dropbox [10], Apple iCloud [2], and Google Drive [18] further provide file sharing and synchronization services among multiple devices and users. The outsourced data storage service provides users convenience and global data accessibility at low cost, and frees them from the burden of maintaining huge local data storage.

Permission to make digital or hard copies of all or part of this work for personal or classroom use is granted without fee provided that copies are not made or distributed for profit or commercial advantage and that copies bear this notice and the full citation on the first page. Copyrights for components of this work owned by others than ACM must be honored. Abstracting with credit is permitted. To copy otherwise, or republish, to post on servers or to redistribute to lists, requires prior specific permission and/or a fee. Request permissions from permissions@acm.org.
CCSW'13, November 8, 2013, Berlin, Germany.
Copyright 2013 ACM 978-1-4503-2490-8/13/11 ...\$15.00.
<http://dx.doi.org/10.1145/2517488.2517494>.

Although there are powerful economic reasons to adopt cloud storage, outsourcing data introduces some potential risks, typically thought of in terms of confidentiality, availability, integrity, and freshness. These risks arise due to many factors, including malicious attacks on the storage provider, insider attacks, administrative mistakes, or traditional hardware failures. Most of these concerns can be resolved by software: confidentiality by encryption, availability by appropriate data replication, and integrity by digital signatures and message authentication codes. On the contrary, it is difficult to ensure freshness in software when there are multiple clients involved.

Freshness requires the data read from a server to match the latest write, and it is difficult to enforce in software because it requires knowing about all possible writes that the server may have acknowledged. With a naïve client that has no client-side mutable state, a malicious server can perform a replay attack by answering the client's read request with properly signed but stale data. This attack can be detected if the client remembers the last operation he/she has performed [23]. In the presence of multiple clients, a server can "fork" its state to prevent one client from seeing another client's writes, and detecting such attacks requires one client to learn about the other client's writes out of band [23].

To detect forking attacks, software-based solutions [6, 33, 24, 12] require user-to-user communication and thus cannot achieve immediate detection. Hardware-based solutions [8, 22, 36], on the other hand, add a piece of trusted hardware to the system. The trusted hardware typically provides a secure log or a monotonic counter, preventing a malicious server from reversing the system state to its previous value or presenting valid but inconsistent system states to different users. However, such trusted hardware is often resource-constrained, and becomes a performance bottleneck.

To improve the performance of trusted hardware while keeping the cost low, Costan et al. in a position paper [9] proposed splitting the functionality of the trusted hardware into two chips: a P (processing) chip and an S (state) chip. The P chip has high computing power to perform sensitive computations, and the S chip has secure non-volatile memory (NVRAM) to store the system state. However, Costan et al.'s design does not address two possible attacks that can violate integrity and freshness guarantees: (1) a server (or other malicious users) can pretend to be a legitimate user and perform unauthorized/replayed writes without being detected, and (2) a server can maliciously discard the users' updates that are already acknowledged by disrupting the P chip's supply power and resetting it with the stale state stored on the S chip. Prior work also does not address the key challenge of crash recovery: a server that crashes before data is written to the disk may be forced to stop providing service altogether, due to the inconsistency between the disk and the state stored on the S chip. Furthermore, to our best

knowledge, neither results nor implementation have been provided to prove whether split trusted hardware achieves high performance.

In this paper, we rectify the security vulnerabilities in the S-P chip model proposed by Costan et al. and provide a detailed design augmented with a precise write access control scheme and system state protection against power loss. In addition, we propose an efficient crash recovery mechanism to improve system reliability. To prove our design achieves high performance while ensuring data integrity and freshness, this paper presents a full-system implementation and end-to-end evaluation of the proposed system for authenticated storage. Our system achieves high throughput by parallelizing the operations carried out on the server and the P chip and permitting the untrusted server to manage caches and schedule disk writes to optimize disk I/O.

We implement our prototype trusted hardware on an FPGA and connect it to a Linux server. A client model is also implemented in Linux and it runs an ext2 file system on top of our authenticated block storage. We demonstrate that (1) our system performance is comparable to that of the Network File System (NFS) [31, 32] and (2) the security mechanisms introduce little performance overhead—around 10% for typical file system benchmark workloads under a realistic network scenario. In addition, we provide customized solutions based on micro-benchmark results: (1) For performance-focused storage providers, our design can achieve 2.4 GB/s throughput using an ASIC paired with a smart card chip; (2) For budget-focused storage providers, our design scales to a single-chip solution that is feasible under today’s NVRAM process and can achieve 377MB/s throughput, which is much higher than that of other existing single-chip solutions [36]. This single-chip solution does not follow the high-level concept proposed in [9].

The main contributions of this work are as follows:

- A detailed design and implementation of a trusted hardware platform that provides integrity and freshness guarantees and achieves high throughput and low latency.
- A state protection scheme that tackles the security vulnerability caused by power attacks on the split trusted hardware.
- A write access control scheme that prevents unauthorized writes from violating integrity and freshness guarantees.
- A crash recovery mechanism to protect the system from accidental or malicious crashes, which both allows the untrusted server to schedule disk writes and still provides strong freshness guarantees.
- An end-to-end evaluation that shows our design introduces little overhead on file system benchmarks.
- A single-chip solution of our prototype is shown to achieve much higher throughput than existing hardware solutions.

The rest of this paper is organized as follows: Section 2 presents the related work. Section 3 provides an overview of our system, and Section 4 describes its design. Implementation details and optimizations are discussed in Section 5. Section 6 evaluates the system performance. Section 7 concludes the paper.

2. RELATED WORK

To ensure data integrity by detecting unauthorized data modification, cryptographic hashes, message authentication codes (MACs), and digital signatures are commonly adopted in current systems [15, 21, 29]. In addition, fine-grained access control is needed to separate the writers from the readers in the same file. For example, in Plutus [21], each file is associated with a public/private key pair to differentiate read/write access. For each file, a private file-sign key

is handed only to the writers, while the readers have the corresponding public file-verify key. When updating the file, an authorized writer recomputes the hash of the file (which is the root hash calculated from the block hashes using the Merkle tree technique [27]), signs the hash with the file-sign key, and places the signed hash in the file header. Then, readers can check the integrity of the file by using the file-verify key to verify the signed hash.

Freshness verification of outsourced storage is more challenging, especially when serving a large number of clients. When issuing a read request to a cloud server, a client cannot detect the server’s misbehavior using the signature verification scheme mentioned above if the server performs a replay attack by maliciously sending the stale data with a valid signature from an authorized user. This kind of attack can cause freshness violations.

In a single-client setting, a replay attack can be detected if the client is aware of the latest operation he or she has performed. Cryptographic hashes can be used to guarantee both integrity and freshness. A naïve approach is to store a hash for each memory block in the client’s local trusted memory and verify the retrieved data against the corresponding hash value. For large amounts of data, tree-based structures [27, 19, 11] have been proposed to reduce the memory overhead of trusted memory to a constant size. In tree-based approaches, the tree root represents the current state of the entire memory, and it can be made tamper-resistant and guaranteed to be fresh if stored in trusted memory. The trusted memory can be the client’s local memory in this case. For example, the Merkle tree technique [27] is commonly used in outsourced file systems [20, 16] to reduce the storage overhead at the client-side to a constant. In our design, we also apply the Merkle tree technique but store the root hash securely at the server side.

In a multi-client system, ensuring freshness is more difficult. In a group collaboration scenario, a cloud server can maliciously prevent each group member from finding out that the other has updated the data by showing each member a separate copy of data. This kind of replay attack is called a forking attack, which was first addressed by Mazières and Shasha in [25, 26]. Mazières and Shasha introduced the forking consistency condition in [26], showing that a forking attack can be detected unless clients cannot communicate with each other and can never again see each other’s updates. The SUNDR system [23] was the first storage system using forking consistency techniques on an untrusted server, and there were subsequent fork-based protocols, such as [7] and [5]. User-to-user communication is required to detect server misbehavior: for example, FAUST [6] and Venus [33] allowed clients to exchange messages among themselves. To improve the efficiency, FAUST weakened the forking consistency guarantee, and Venus separated the consistency mechanism from storage operations and operated it in the background. Depot [24] and SPORC [12] further supported disconnected operations and allowed clients to recover from malicious forks. In addition to storage services, forking consistency has been recently applied to a more general computing platform [4].

Software approaches mentioned above allow totally untrusted servers and rely on end-to-end checks to guarantee integrity. Although some software solutions can detect and even recover from malicious forks, they require communication among clients and therefore cannot detect attacks immediately. Hardware solutions, on the other hand, use trusted hardware as the root of trust to provide stronger security guarantees as compared to software-only approaches and simplify software authentication schemes.

To immediately detect forking attacks, a piece of trusted hardware is used as a trusted computing base (TCB) and attached to the system. Critical functionality is moved to the TCB to ensure trustworthiness. The Trusted Platform Module (TPM) [35], a low-cost

tamper-resistant cryptoprocessor introduced by the Trusted Computing Group (TCG), is an example of such trusted hardware. Since TPMs became available in modern PCs, many researchers have developed systems that use the TPM to improve security guarantees.

Attested append-only memory (A2M) proposed by Chun et al. [8] provided the abstraction of a trusted log that can remove equivocation and improve the degree of Byzantine fault tolerance. Van Dijk et al. used an online untrusted server together with a trusted timestamp device (TTD) implemented on the TPM to immediately detect forking and replay attacks [36]. Levin et al. proposed TrInc [22], which is a simplified abstraction model and can be implemented on the TPM. In both TrInc and TTD, monotonic counters were used to detect conflicting statements sent from the untrusted server to different clients.

Trusted hardware designed for these secure storage services requires secure NVRAM for long-term storage as well as control logic and cryptographic engines. However, it is difficult to achieve high-performance computation while keeping cost low by combining all the building blocks on a single chip, because the silicon fabrication technology for the NVRAM and that for high-performance computational logic are different. Therefore, today’s trusted hardware is generally slow, which affects the throughput and latency of the whole system. To avoid this problem, Costan et al. proposed splitting the functionality of the TCB into two chips: a P chip with high throughput and an S chip with secure NVRAM [9]. The P chip and S chip are securely paired to serve as a single TCB. Compared to previous single-chip solutions, this two-chip model allows trusted hardware to perform more complicated operations without performance degradation. However, Costan et al. did not address potential power attacks on the split trusted hardware, and the proposed system was vulnerable to unauthorized writes that can cause integrity and freshness violations.

In this work, in order to immediately detect forking attacks and minimize the clients’ workload, we place the trusted components at the server side. To enhance efficiency, as suggested in [9], we use an S-P chip pair as the TCB model in our prototype system. To rectify the security vulnerabilities in the previous S-P chip model, we propose a freshness-guaranteed write access control, a state protection scheme, and a crash-recovery scheme to deal with unauthorized/replayed writes and power loss events. Finally, we provide a detailed evaluation showing that we can significantly reduce overheads caused by security checks on trusted hardware, and increase the capabilities of trusted storage systems, e.g., the number of clients and bandwidth, significantly beyond [36, 22].

3. GOALS AND OVERVIEW

To build a practical cloud storage system that can immediately detect integrity and freshness violations, our design should achieve the following goals: (1) Integrity and freshness guarantees, (2) Simple data checking and management done by clients, (3) Simple API (single request/response transaction per operation) between the server and its clients, (4) Little local storage, (5) Acceptable overhead and cost, and (6) Customized solutions in which storage providers are able to adjust their systems according to the performance and cost trade-off.

3.1 System Overview

To build a trusted cloud storage system that efficiently guarantees integrity and freshness of cloud data, we attach a piece of trusted hardware to an untrusted server and adopt the S-P chip model as the trusted hardware; that is, the functionality of the trusted hardware is split into S and P chips. The P chip, which can be an FPGA board or an ASIC, has high computing power but only volatile memory,

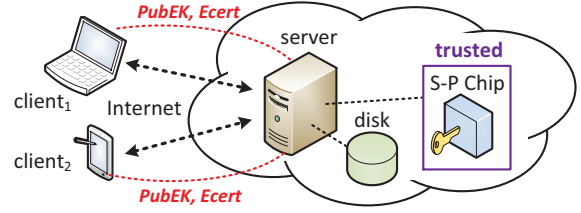


Figure 1: System model

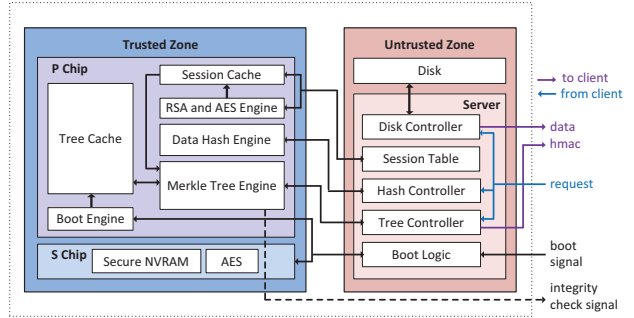


Figure 2: Design overview

while the S chip, which can be a smart card, has secure NVRAM but only constrained resources.

Figure 1 represents the system model. For simplicity, we make an assumption that a single-server system provides its clients with a block-oriented API to access a large virtual disk. The clients access the cloud storage service via the Internet; the untrusted server is connected to the disk and the trusted S-P chip pair.

To access/modify the cloud data, the clients send read/write requests, wait for the responses, and then check data integrity and freshness. The untrusted server schedules requests from the clients, handles disk I/O, and controls the communication between the P chip and S chip. The S-P chip pair shares a unique and secret HMAC key with each client, and thus essentially becomes an extension of the clients. The S-P chip pair is trusted to update and store the system’s state, manage write access control, verify data integrity, and authenticate the responses sent to the client using the HMAC key. More specifically, the P chip performs all of the sensitive computations and stores the system’s state when the system is powered, and the S chip securely stores the system’s state across power cycles. This scheme simplifies the computation and verification that need to be done by clients in software-based solutions, and abstracts away the design complexity and implementation details.

3.2 Threat Model

In our system model shown in Figure 1, the cloud server is untrusted: it may answer the clients’ read requests with stale or corrupted data, and it may pretend to be a client and overwrite the client’s data. The server may maliciously crash and disrupt the P chip’s supply power to drop the clients’ recent updates. The disk is vulnerable to attackers and hardware failures, so the data stored on the disk may not be correct. All connection channels within the system (including the communication between the S and P chips) are also untrusted. Any message traveling on the channels may be altered to an arbitrary or stale value. A client is trusted with the data he/she is authorized to access, but the client may try to modify the data outside the scope of his/her access privilege.

Table 1: Notation

Notation	Description
$H(X)$	the hash value of X
$\{M\}_K$	the encryption of message M with the key K
$HMAC_K(M)$	the HMAC of message M with key K
MT_{XYN}	the message type indicating that a message is sent from X to Y with sub-type N

This work allows clients to identify the correctness of the responses sent from the server. If the received response is incorrect, the client will not accept it and will resend the original request or report the event to the system manager. Therefore, receiving an incorrect response can be considered as a missing response and can be treated as a denial-of-service attack, which falls out of the scope of this work.

3.3 Chain of Trust

The S chip and P chip are securely paired during manufacturing time and thus can be seen as a single TCB. The two chips share an endorsement key pair ($PubEK, PrivEK$) and a symmetric encryption key SK . The manufacturer, who can be seen as a CA, signs $PubEK$ and produces the endorsement certificate ($ECert$) to promise that $PrivEK$ is only known to the S-P pair. Our S-P pairing procedure is similar to that described in [9]. We use the S-P chip pair as the root of trust and establish the chain of trust, allowing clients to trust the computation and verification performed by our storage system.

When a client connects to the cloud server, $ECert$ (and $PubEK$) is presented to the client for verification. If the verification is successful, which means $PubEK$ can be trusted, the client can secretly share an HMAC key with the S-P chip pair by encrypting the HMAC key under $PubEK$. The S-P chip pair can then use the HMAC key to authenticate the response messages sent to the client.

In this work, we also provide a single-chip solution where the S chip and P chip are integrated into an ASIC. This chip can be viewed as a smart card running at a higher frequency with additional logic for data hashing. The detailed specification is described in Section 6.3.2. In this solution, the communication between the S and P chips becomes on-chip and can be trusted, so the pairing scheme is no longer required. This single chip also generates ($PubEK, PrivEK$) and SK at manufacturing time and follows the chain of trust model described above.

4. DESIGN

Figure 2 represents our prototype system architecture, which consists of two parts: an untrusted server with an untrusted disk, and a trusted S-P chip pair. This section introduces our system’s characteristics and describes how we achieve the security and performance goals. The detailed hardware mechanisms are discussed in Section 5. Table 1 lists the symbols used in our design concepts and protocols. More details about our exact protocol are provided in a separate technical report [37].

4.1 Memory Authentication

To verify the integrity and freshness of the disk data, we build a Merkle tree [27] on top of the disk (see Figure 3). The hash function’s collision resistance property allows the Merkle tree root, which is also called the root hash, to represent the current disk state. The root hash is calculated and stored in the S-P chip pair, so it can be trusted against any corruption or replay attacks. The root hash is guaranteed to be always fresh, and leaf hashes are verified

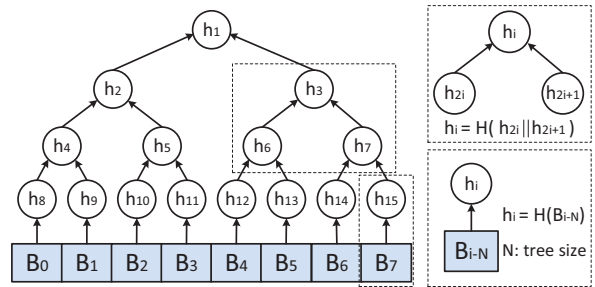


Figure 3: A Merkle tree example for a disk with 8 blocks

by the S-P chip pair to be consistent with the root hash and sent to the clients in the response messages, which are authenticated using HMACs. Therefore, a client can detect any data corruption or forking attack by verifying the received data against the received leaf hash. There is no need to communicate with other clients to check the data consistency.

To improve the efficiency of the Merkle tree authentication, we let the P chip cache some tree nodes. The caching concept is similar to what Gassend et al. proposed in [13]: once a tree node is authenticated and cached on-chip, it can be seen as a local tree root. While Gassend et al. use the secure processor’s L2 cache, which is on-chip and assumed to be trusted, to cache tree nodes, we cache the tree nodes on the P chip and let the untrusted server control the caching policy. This is because software has much higher flexibility to switch between different caching policies in order to match the data access patterns requested by various cloud-based applications.

In our prototype system, the entire Merkle tree is stored on the untrusted server. The P chip caches tree nodes; its Merkle tree engine (see Figure 2) updates the cached nodes to reflect write operations and verifies the tree nodes to authenticate read operations.

The Merkle tree engine manages the cached nodes according to the commands sent from the server’s tree controller, which controls the caching policy. There are three cache management commands: (1) the LOAD command asks the tree engine to load a certain tree node and evict a cached node if necessary; (2) the VERIFY command asks the tree engine to authenticate two child nodes against their parent node; (3) the UPDATE command asks the tree engine to calculate and update the tree nodes on a certain path from a leaf node to the root. These commands are sent from the untrusted server; therefore, the tree engine performs additional checks for each command to prevent integrity and freshness violations. If any verification step fails, the integrity check signal is raised to report the error to the system manager.

4.2 Message Authentication

We use the HMAC technique to create an authenticated channel over the untrusted connection between each client and the trusted S-P chip pair. Requests/responses are verified with HMACs to prevent message corruption or replay attacks. Each HMAC key should be only known to the client and the S-P chip pair.

Figure 4 describes how we securely share the HMAC key between a client and the S-P chip pair with minimal performance overhead even when the system serves multiple clients. The client and server communicate via a session-based protocol.

Each time a client connects to the server, the client first requests a session. Each session has a unique HMAC key, so an HMAC key is also called a session key ($Skey$). To share $Skey$ with the S-P chip, the client encrypts $Skey$ with $PubEK$ and sends it along with the request for a new session. Then server assigns a new session ID

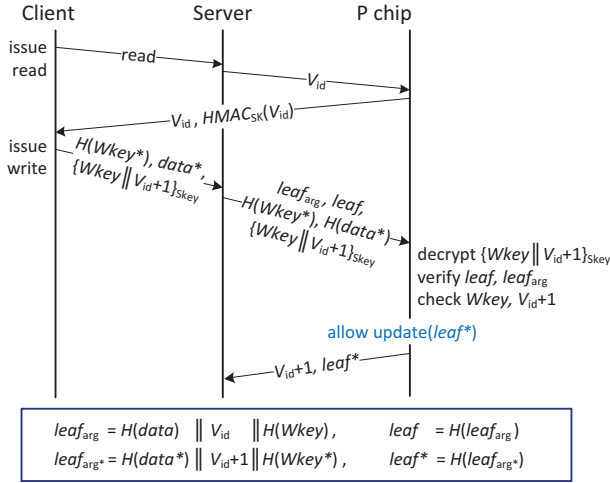


Figure 5: Write access control example

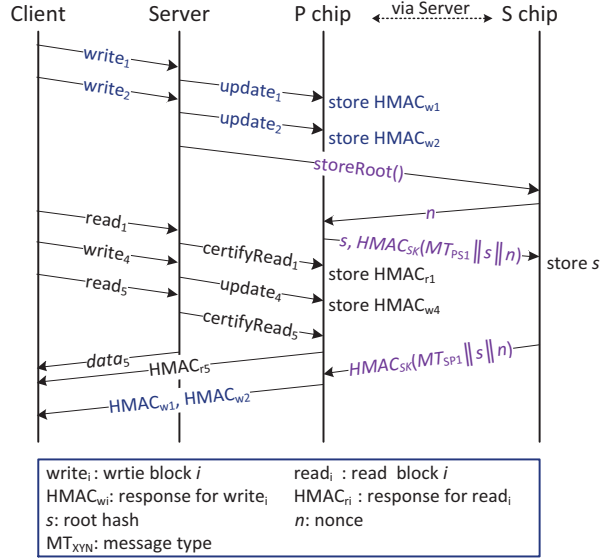


Figure 6: Root hash storage protocol

detect the inconsistency. Considering that the S chip has long write times (around 1 ms/byte for smart cards [30]), in order to maintain high throughput, the P chip handles the clients' new requests but stores the responses in an on-chip buffer while waiting for the S chip's acknowledgment of successfully saving the root hash.

Figure 6 illustrates our root hash storage protocol. After a Merkle tree update, the P chip generates an HMAC to authenticate the write operation, stores the HMAC in the on-chip buffer instead of sending it to the client immediately. When receiving the server's storeRoot() request, the S chip sends a random nonce (*n*) to the P chip, and the P chip sends the latest root hash (*s*) to the S chip. While waiting for the S chip's acknowledgment, the P chip keeps handling clients' requests and generating responses (HMAC_{wi} and HMAC_{ri}). The P chip stores the responses that are used to authenticate write operations or read operations that access the same blocks written by buffered write operations. The P chip releases the responses only if it receives a valid acknowledgment from the S chip indicating that the corresponding root hash has been successfully stored.

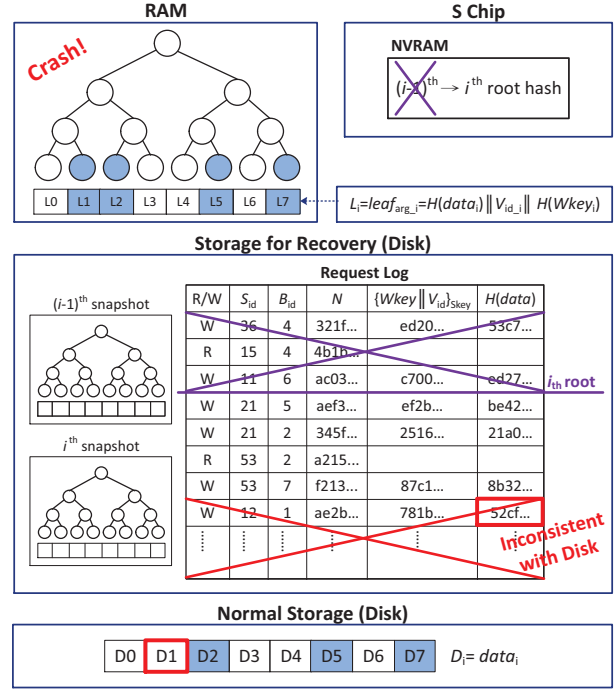


Figure 7: Crash-recovery mechanism

In the two-chip prototype system, communication between the S chip and P chip is via server and thus untrusted. To securely store the latest root hash on the S chip, after the P chip receives the nonce *n* from the S chip, it sends out $HMAC_{SK}(MT_{PSI} || s || n)$ along with the root hash *s*, and the S chip uses $HMAC_{SK}(MT_{SPI} || s || n)$ as the acknowledgment, where MT_{PSI} and MT_{SPI} are message types used to distinguish the HMACs sent by the P chip and by the S chip so that the server cannot maliciously acknowledge the P chip. In a single-chip solution, the communication between the S and P chips becomes trusted, and hence the HMACs for the root hash storage protocol are no longer needed.

4.5 Crash-Recovery Mechanism

The crash-recovery mechanism ensures that even if the server accidentally/maliciously crashes, the disk data can be recovered to the state that is consistent with the root hash stored on the S chip.

There are two possible scenarios in which the disk state after the server re-boots is not consistent with the root hash stored on the S chip. One happens when the server crashes after the root hash is stored on the S chip but the data has not yet been stored on the disk. The other one happens when the server crashes after the data is stored on the disk but the corresponding root hash has not yet been stored on the S chip. To prevent the first scenario, the server should first flush the data into disk before it passes the root hash to the S chip, eliminating the possibility that the root hash is newer than the disk state. To recover from the second scenario, we keep a request log on the disk where we save a snapshot of the Merkle tree leaf arguments ($H(Wkey), V_{id}, H(data)$ for each block).

Figure 7 shows how the recovery scheme works. When the server sends out a storeRoot() command and obtains the latest root hash (*i*th root hash) from the P chip, it flushes data into the disk, takes a snapshot of the current Merkle tree leaf arguments (*i*th snapshot) and stores it on the disk. After the data and snapshot are stored on the disk, the server sends the root hash to the S chip and continues

Table 2: API between client and server

Command	Client Arguments and Server Responses
connect()	Args: None Resp: $PubEK, ECert$
createSession()	Args: $\{Skey^a\}_{PubEK}$ Resp: Sid^b
readBlock()	Args: $Sid, Bid^c, n^d, HMAC(reqR)^e$ Resp: $data, Vid^f, HMAC(respR)^g$
writeBlock()	Args: $Sid, data, H(data), \{Wkey Vid\}_{Skey}$ $Bid, n, H(Wkey^*), HMAC(reqW)^h$ Resp: $HMAC(respW_1)^i$ if write succeeds; $Vid^*, HMAC(respW_2)^j$ if invalid Vid
closeSession()	Args: Sid Resp: None

^a HMAC Key ^b Session ID ^c Block ID ^d Nonce

^e $HMAC_{Skey}(MT_{CP0}||Bid||n)$ ^f Revision number

^g $HMAC_{Skey}(MT_{PC0}||Bid||n||H(data)||Vid)$

^h $HMAC_{Skey}(MT_{CP1}||Bid||n||H(data)||H(Wkey^*))$

ⁱ $HMAC_{Skey}(MT_{PC1}||Bid||n||H(data))$

^j $HMAC_{Skey}(MT_{PC2}||Bid||n||Vid)$

to handle clients' new requests. The Merkle tree and access information stored in the RAM are updated by new write requests. The request log buffers all the requests whose responses are buffered by the P chip without storing any actual write data. Note that we also keep the previous snapshot ($(i-1)^{th}$ snapshot) on disk so that the system is able to recover from a crash that happens after the server sends the root hash but before the root hash is successfully stored. When the server receives the S chip's acknowledgment saying that the i^{th} root hash is successfully stored, it clears all the requests that are not newer than the i^{th} root hash from the request log.

When the server reboots after crashes, it first re-loads the snapshots, re-builds the two Merkle trees, and chooses the one that is consistent with the S chip's root hash. Then, the server re-performs the requests in the request log until the root hash is consistent with the disk state. If the untrusted server fails to correctly perform this crash-recovery mechanism, the clients will be able to detect the inconsistency between the disk state and the state stored on the S chip when they issuing read requests. We assume that each write of a data block is atomic; that is, the file system guarantees that writing the whole amount of data within one data block is not interrupted.

4.6 Trusted Storage Protocol

Table 2 shows the API between each client and the server. In the following we describe how the components in our system work together to provide a trusted storage service.

When the cloud server boots, the server's boot logic re-pairs the S chip and P chip and executes the recovery procedure if the server re-boots from a crash. When a client requests a new session, the server assigns a new session ID (Sid) to the client and stores the client's HMAC key ($Skey$) as described in Section 4.2. After the session is created, the client uses Sid to communicate with the storage system, sending read/write requests to access/modify the data. For a read request, the server reads disk data and asks the P chip to verify the Merkle tree nodes and to generate an HMAC for authentication. As described in Section 4.4, the P chip buffers the HMAC if the client tries to access the data that is not yet reflected by the S chip's root hash. For a write request, the P chip checks the client's write access and only allows authorized users with a correct revision number to update the Merkle tree (see Section 4.3). The

Table 3: P chip implementation summary

Modules	FFs	LUTs	Block RAM/FIFO
Data Hash Engine	4408	5597	0 kB
Merkle Tree Engine	4823	9731	2952 kB
Ethernet Modules	1130	1228	144 kB
Total	10361	16556	3096 kB

server writes the data into the disk and asks the P chip to send the latest root hash to the S chip. The P chip buffers the HMAC for the write operation until the root hash is successfully stored on the S chip. At the same time, the server stores the required information on the disk as described in Section 4.5 so that the system is able to recover from crashes.

5. IMPLEMENTATION

In this section, we present the implementation details of our prototype system. To evaluate the system performance and overhead introduced by security mechanisms, we implement the client and server on Linux platforms. The client and server communicate over TCP, and both of them are running at user-level. The P chip is implemented on an FPGA board, which connects to the server using Gigabit Ethernet. To increase the implementation efficiency while maintaining the evaluation accuracy, the timing and functionality of the S chip are modeled by the server. For convenience, we refer to the implemented system as ABS (authenticated block storage), which consists of an ABS-server and an ABS-client.

5.1 P Chip Implementation

We implemented the P chip on a Xilinx Virtex-5 FPGA, using Gigabit Ethernet to connect with the server. Inside the P chip (see Figure 2), the AES engine, data hash engine, and Merkle tree engine can be executed in parallel while sharing a single Ethernet I/O. The implementation of the boot engine and the session cache can be safely omitted and modeled by the server because they only introduce constant overhead per reboot or per session.

The AES engine [3] is mainly designed for symmetric decryption of the client's write access information used in our write access control protocol (see Section 4.3), which requires one symmetric decryption and two hash calculations to be performed on the P chip. The AES engine can also be reused for the boot process and the HMAC key decryption. The data hash engine is used to verify the integrity of data sent from a client by checking the computed hash against the hash sent from the client. We implemented a 4-stage pipelined SHA-1 engine ([34]) for performance reasons. This hash engine can also be replaced by a software hash function without degrading the security level when hardware resources are limited. If the server mis-computes the hash and allows the wrong data to be stored on disk, the inconsistency can be detected by the client on the next read to the same block. The Merkle tree engine uses another pipelined hash engine to perform hash verifications and tree updates. The tree engine can pipeline multiple tree updates on different update paths (while the update steps on the same path need to be serialized) and reduce the number of hash operations by merging the hash operation performed by sibling nodes. Table 3 shows a summary of the resources used by the P chip.

5.2 S Chip Implementation

The S chip has fixed and limited functionality and thus has little space for performance optimization. Therefore, for simplicity, instead of implementing the S chip on a smartcard, we modeled its functionality and timing on the server. The speed of the S chip can

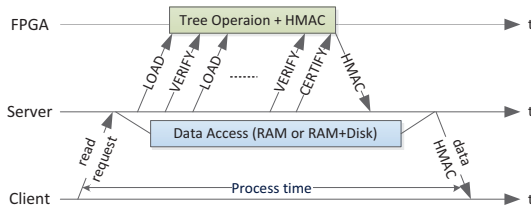


Figure 8: Timeline of a read operation

affect the system latency overhead because of the root hash storage protocol (see Section 4.4), which requires the P chip to buffer the responses of the write operations and related read operations until the latest root hash is stored on the S chip. The latency overhead depends on the issuing rate of the server’s storeRoot() requests and the round-trip time, which consists of the time the server spends on flushing the data to disk, the time the S chip spends on storing the 20-byte root hash (around 20ms), checking and generating HMACs (around 2ms if using a 32-bit RISC CPU or less time if using a SHA-1 hardware engine). To evaluate the root hash storage protocol, the modeled S chip sends back the acknowledgment 22ms after it receives the latest root hash.

5.3 Server Implementation

We built the server on Linux. As shown in Figure 2, the data controller handles disk accesses; the hash controller and tree controller send commands via the Ethernet controller to control the computation on the P chip. The server schedules operations following the trusted storage procedure described in Section 4.6. To achieve parallel execution, we put the data controller on another thread.

Figure 8 shows the timeline of a read operation. When receiving a read request, the server reads the data from the disk or the buffer cache. Meanwhile, the server sends the tree operation commands to the FPGA and asks the FPGA to generate an HMAC for authentication. After the server receives the data and HMAC, the server sends them to the client and starts to handle the next request.

When handling a write operation, the server checks the integrity of data sent from the client by re-computing the hash of data and checking against the client’s data hash before the server writes the data to disk. To minimize the latency, we perform speculative writes: the server writes the data into the buffer cache in parallel with the hash engine operation. If the verification fails, the data in the buffer cache should be discarded. The operating system should be modified so that it only writes correct data blocks to the disk.

Figure 9 shows the timeline of a write operation. When receiving a write request, the server sends the client’s data and encrypted write access information ($\{Wkey||V_{id}\}_{Skey}$) to the FPGA; in the meantime, the server writes the data into the buffer cache. After the data and write access information are verified, the server sends tree cache commands to the FPGA and data to the disk. The P chip generates and buffers the write response (HMAC) until receiving the root hash storage acknowledgment from the S chip. The server schedules the root hash storage protocol by sending out storeRoot() requests and forwarding the root hash from the P chip to the S chip after the data and Merkle tree snapshot are stored on the disk. Since the disk write controlled by the operating system can be done in the background, the next request can be handled once the server finishes writing the data to the buffer cache and the FPGA finishes generating the HMAC. Therefore, in general, the disk write time (as well as the S chip write time) does not affect the system throughput if the P chip’s response buffer is large enough.

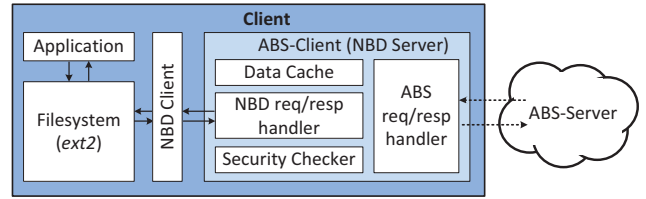


Figure 10: The client model

The throughput and latency of the buffer cache can be seen as the optimal performance our system can achieve, since all data sent from the server or from the disk must pass through the buffer cache. If there is a perfect caching scheme and a sufficient number of hard disks, then the disk read time will be close to the RAM access time, and disk write time will not affect the system throughput but only introduce a constant latency. In Section 6.1, we measure the optimal system throughput by measuring the data access time to/from the buffer cache when running micro-benchmarks. Instead of modifying the operating system, we store all test data in a RAM buffer, which mimics the buffer cache with a 100% hit rate. In Section 6.2, we evaluate our system using a real disk and analyze the disk impact on system latency when running file system benchmarks.

5.4 Client Implementation

To allow end-to-end evaluation that takes the network latency and throughput into account (see Section 6.2), we implemented a client model as shown in Figure 10. User applications are running on top of the ext2 filesystem that is mounted on a network block device (NBD). When a user-program accesses the filesystem, the NBD client forwards the request to the ABS-client, which processes and sends the request to ABS-server, where the data physically resides.

The communication between the ABS-client and ABS-server follows the client-server API described in Table 2. To amortize the overhead introduced by security mechanisms, ABS prefers block sizes that are larger than the block size of a typical filesystem. For example, in our evaluation, we fix the block size of ABS as 1 MB, while ext2 uses 4 KB blocks. To handle requests in different block sizes, the ABS-client merges continuous reads and writes to eliminate redundant requests to the ABS-server and adds read-modify-writes to deal with partial writes. To further optimize the performance of large block sizes, we keep a 16 MB local write-through cache in the ABS-client and allow partial write data with the hash of the whole block to be sent to the server.

6. EVALUATION

This section evaluates the throughput and latency of our prototype system. The performance overhead introduced by providing integrity and freshness guarantees is analyzed. We also provide suggestions on hardware requirements for different storage providers.

To conduct our experiments, the ABS-server program runs on an Intel Core i7-980X 3.33 GHz processor with 6 cores and 12 GB of DDR3-1333 RAM. The ABS-server computer connects with a Xilinx Virtex-5 XC5VLX110T FPGA board and an ABS-client computer, which is an Intel Core i7-920X 2.67 GHz 4 core processor, via Gigabit Ethernet. The client-server connection can be configured to add additional latency and impose bandwidth limits.

In our experiments, we fix the disk size as 1 TB and block size as 1 MB, which is close to the block sizes used in current cloud storage system. For example, Dropbox uses 4 MB blocks, and the Google

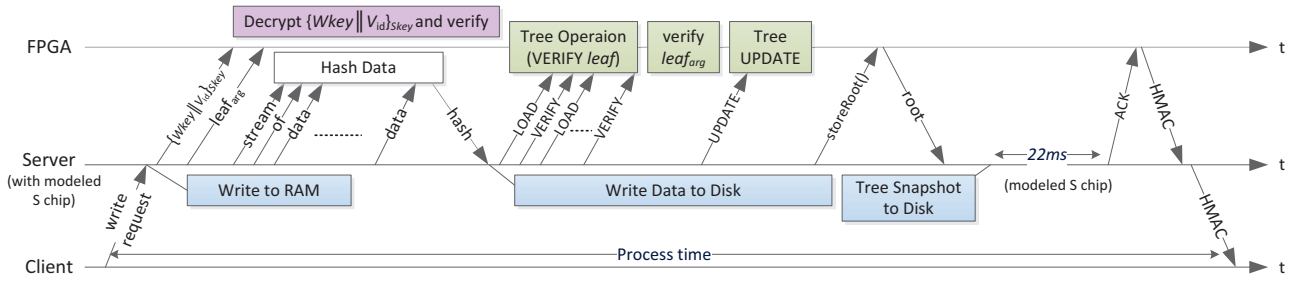


Figure 9: Timeline of a write operation

Table 4: Micro-benchmarks

Benchmark Type	Description
read/write only cont	sequentially read/write 2 GB
read/write only period	sequentially read/write the same 256 MB space 8 times
read only random	randomly read from 2 GB
write only random	randomly write from 2 GB
random read write	randomly read or write from 2 GB (read probability = 0.8)

Table 5: Detailed timing analysis (in ms)

Benchmark		Data Access	Hash	Tree + HMAC
read only random	Baseline	4.01E-1	0	1.69E-3
	ABS-SOFT	3.93E-1	0	2.02E-2
	ABS-HARD	3.97E-1	0	2.04E-2
write only random	Baseline	1.76E-1	2.29	2.40E-3
	ABS-SOFT	1.74E-1	2.33	3.72E-2
	ABS-HARD	1.69E-1	9.51	3.69E-2

Table 6: ABS performance summary

Configuration		ABS-SOFT	ABS-HARD
Randomly Write	Throughput	411 MB/s	104 MB/s
	Latency	2.4 ms	12.3 ms
Randomly Read	Throughput	2.4 GB/s	
	Latency	0.4 ms	

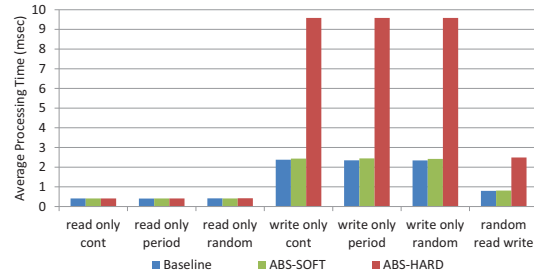


Figure 11: Average processing time comparison ^a

^a2048 operations on 1 MB data blocks with tree cache size = 2¹⁴

File System uses 64MB chunks [14]. For a storage provider, the best choice of the block size depends on its clients' access patterns.

6.1 Micro-Benchmarks

To analyze the overhead introduced by the memory authentication scheme and the maximum throughput that the ABS-server can provide, we built another system assuming the server is trusted and refer to it as Baseline. Baseline-server is trusted to generate HMACs and perform all the authentication and permission checks. We run micro-benchmarks (listed in Table 4) on the Baseline-server and ABS-server and then compare their performance. To measure the throughput upper bound, two servers were simplified by removing the real disk as well as the root hash storage protocol and crash-recovery mechanism that are affected by the S chip and the disk write time. As mentioned in Section 5.3, we store all the test data in the RAM buffer and measure the data access time to/from the RAM buffer. Both the RAM buffer size and the working set size are set as 2GB.

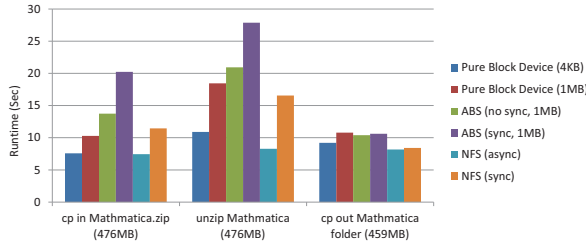
We compare the performance of the Baseline and ABS in terms of average processing time, which is measured from when the server dequeues a request until when the server finishes processing it. In Table 4, in addition to the random accesses, the continuous data accesses simulate backup applications for a single client, while the repeated data accesses simulate group collaboration on the same chunk of data.

Figure 11 shows the processing time comparison between the Baseline and ABS with two configurations: using a hardware data hash engine (ABS-HARD) or a software hash (ABS-SOFT). The three schemes have the same performance when handling reads, while ABS-HARD is four times slower when handling writes. To understand which component slows down the system, we performed detailed timing analysis as shown in Table 5. When handling reads, the processing time is equal to the data access time. The latency of Merkle tree and HMAC operations is completely hidden because they are fast enough and can be executed in parallel with data access. When handling writes, the hash operation dominates the processing time and introduces large overhead in ABS-HARD because the throughput and latency of the hash engine are limited by the Ethernet connection, which has the throughput of 125MB/s.

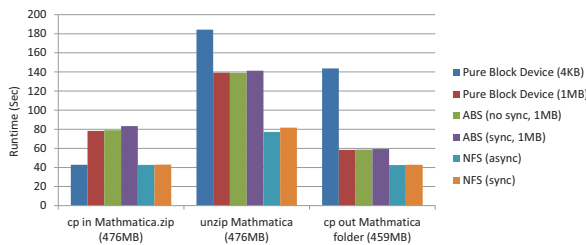
Table 6 shows the performance of ABS-SOFT and ABS-HARD. The hash engine in our prototype hardware has lower throughput and higher latency due to the limitation of Ethernet I/O, and it runs at a much lower clock frequency (125 MHz, which is also limited by the Ethernet speed) compared to that of the software hash function (3.33 GHz). However, in a real storage system, these limitations can be easily removed by using an ASIC as the P chip. The clock frequency can be increased to 500MHz or 1 GHz, and a faster data bus, such as PCI Express x16, can be used. Moreover, it is cheaper and more energy-efficient to have multiple hash engines in hardware to achieve throughput higher than that of software hash function.

Table 7: Modified Andrew Benchmark (in sec)

	Slow Network	Fast Network
Pure Block Device (4KB)	19.98	10.05
Pure Block Device (1MB)	17.70	10.48
ABS (no sync, 1MB)	17.32	11.27
ABS (sync, 1MB)	24.31	13.76
NFS (async)	72.20	2.35
NFS (sync)	95.12	21.35



(a) Fast network with 0.2ms latency and 1Gbit/s bandwidth



(b) Slow network with 30.2ms latency and 100Mbit/s bandwidth

Figure 12: Runtime comparison on the Mathematica benchmark

6.2 File System Benchmarks

In addition to micro-benchmarks, which are used to measure the maximum system throughput and analyze the overhead introduced by the security checks at the server side, we performed end-to-end evaluation that takes client side overhead and network latency/bandwidth into account. During our end-to-end evaluation, all security protocols are active and implemented as described in detail in Section 4 and 5. A real disk is used to analyze the impact of disk access time on the full system latency, and the S chip is simulated in software with a modeled response time.

We focus on two kinds of practical workloads: (1) copying and unzipping an Mathematica 6.0 distribution, which represent reading and writing large files; (2) the Modified Andrew Benchmark (MAB) [28], which emulates typical user behavior. We ran two benchmarks on two network models, representing different scenarios when the authenticated storage server can be used. First, we ran benchmarks on the client-server network without imposing any latency or bandwidth limitations. The measured latency and bandwidth are 0.2ms round-trip and 986Mbit/s. We refer to this network as the fast network, which models the situation where both the ABS-client (which can be an application server) and the ABS-server are inside the data center. In addition to the fast network, we use *tc* (traffic control) to impose 30ms round-trip delay and 100Mbit/s bandwidth limitation to the network. The resulted network has measured 30.5ms latency and 92Mbit/s bandwidth, and it is referred as the slow network. The slow network setting models

Table 8: Hardware requirements

Demand Focused	Performance	Budget
Connection	PCIe x16(P)/USB(S)	USB
Hash Engine	8 + 1 (Merkle)	0 + 1 (Merkle)
Tree Cache	large	none
Response Buffer	2KB	300B

Table 9: Estimated performance

Demand focused	Performance	Budget	
Randomly Write	Throughput	2.4 GB/s	377 MB/s
	Latency	12.3+32ms	2.7+32ms
Randomly Read	Throughput	2.4 GB/s	
	Latency	0.4ms	
# HDDs supported	24	4	

the situation where the ABS-server is in a remote data center, and the client is connecting over the Internet, from a corporate network or a fast home network (like Google Fiber).

Figure 12 and Table 7 show how ABS (which is ABS-SOFT) performs compared to a pure block device. To analyze the overhead of the crash-recovery mechanism, we include 2 ABS configurations: ABS (no sync, 1MB) buffers responses every 22ms, which is the modeled S chip write time; ABS (sync, 1MB) forces data synchronization to the disk before it sends the root hash to the S chip. In Mathematica benchmarks (see Figure 12), benchmark *cp-in* writes a large zip file into the filesystem; *unzip* unzips the file inside the filesystem; *cp-out* copies the entire folder to somewhere outside the filesystem, resulting in pure reads. Compared with the pure block device, which does not include any security checks, with the same block size (1MB), ABS has the same read performance. The average overhead is reduced from 40% to 10% when switching from the fast network to the slow network, because the overhead introduced in write operations (especially due to data synchronization) is mostly hidden by the long network latency.

We also ran benchmarks on a pure block device with 4KB block size to show how the choice of block sizes affects system performance. The system with the small block size performs well on the fast network but has much worse performance on the slow network when reading files. This is because the performance of reads is directly affected by the long network latency, and the system with the large block size takes advantage of spatial locality by caching a few blocks locally.

In Figure 12 and Table 7, we also compared the ABS performance with two NFS configurations: NFS (async) and NFS (sync), where NFS (sync) forces data synchronization before the server sends back responses. NFS manages data at the file level; therefore, it has the best performance when handling few large files (Mathematica benchmarks). When handling many small files (MAB), NFS performs worse, especially on the slow network, because per file overheads dominate the execution time.

6.3 Suggestions on Hardware Requirements

Based on the micro-benchmark results of our prototype system, we provide two different hardware suggestions to cloud storage providers with different needs. We list the different hardware requirements for performance-focused and budget-focused storage providers in Table 8, and the estimated performance is listed in Table 9. The estimated performance is derived from our experiment settings and micro-benchmark results. 32ms additional write latency is modeled by the combination of disk write time and the

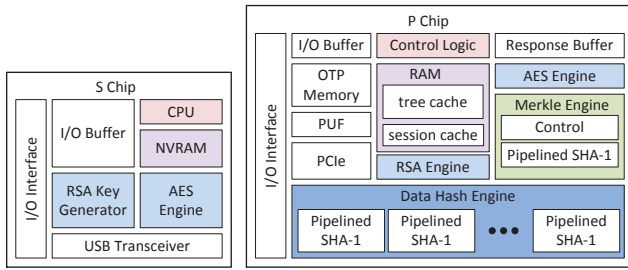


Figure 13: Performance-focused (two-chip) solution

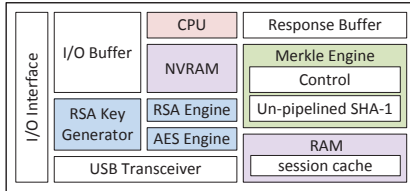


Figure 14: Budget-focused (single-chip) solution

S chip write time, which are introduced by the root hash storage protocol and the crash-recovery mechanism.

6.3.1 Performance-focused Solution

If a storage provider focuses on performance, our system can achieve a throughput as high as its RAM throughput, which is 2.4GB/s, using multiple hardware data hash engines and a fast data bus. The throughput of a pipelined hash engine, 330MB/s, is measured using a mimic fast data bus which has $4\times$ higher throughput than the Gigabit Ethernet. The higher throughput is modeled by only sending a quarter of each 1MB block to the FPGA and expanding it at the FPGA side. To achieve 2.4GB/s throughput of data hashing, we need 8 pipelined hash engines and a PCI Express $\times 16$ link, which supports up to 4.0GB/s. Figure 13 shows the functional units of a S-P chip pair required by a performance-focused storage provider. A typical solution is an ASIC paired with a smart card chip. If the P chip’s computation logic runs at a clock frequency higher than 125MHz, which is easy for an ASIC to achieve, the system latency and the number of hash engines required can be further reduced. For example, for an ASIC running at 500MHz, only 2 data hash engines are required and the system latency can be lower than 3+32ms. In addition, to maintain high throughput under the root hash storage protocol and crash-recovery mechanism, the P chip require a larger on-chip buffer to buffer write responses.

6.3.2 Budget-focused Solution

If a storage provider has limited resources, a solution with a software hash function and without a tree cache can be chosen to reduce the cost while maintaining the system’s throughput around 400MB/s for write requests and 2.4GB/s for read requests (shown in Table 9). We have simulated ABS-SOFT without a tree cache and observed that although the latency of tree operations was ten times larger, there was no significant overhead in the system latency. This is because the latency of tree operations is much smaller than that of other components.

In a budget-focused design, many functional units and on-chip storage are removed. Therefore, we can combine the functionality of the original two chip solution and build a single chip as shown in Figure 14. This single chip can be imagined as a typical smart card chip running at around 125MHz with an additional hardware hash

engine as well as some control logic and a on-chip buffer. In addition, the on-chip communication is trusted, so the HMACs between the original two chips are no longer needed, which makes updating the root hash in the NVRAM easier. Under today’s NVRAM process, this single chip design is feasible in terms of chip area and speed. Therefore, this represents a cheap solution for trusted cloud storage, and yet is significantly more efficient than, for example, the solution of [36].

However, the maximum frequency of this single chip is limited by the NVRAM fabrication process. It is difficult for any logic on chip to run at a frequency higher than 1GHz under today’s NVRAM process, and therefore PCI Express cannot be supported. Given limited frequency, the maximum system system throughput is limited by the communication throughput. For example, the hardware hash engine with 1Gbps communication throughput limits the system throughput to 125MB/s, no matter how many hash engines we have. This is also why we adopt software hashing, which has a limited throughput as 377MB/s, in the single chip solution. On the other hand, the two-chip solution can break this frequency limit and achieve higher throughput as we provide in the performance-focused solution.

7. CONCLUSION

In this work, we provide a detailed design and implementation of an authenticated storage system that efficiently ensures data integrity and freshness by attaching a trusted pair of chips to an untrusted server. We propose a write access control scheme to prevent unauthorized/replayed writes and introduce a crash-recovery mechanism to protect our system from crashes. With micro-benchmarks, we show that even with limited resources the system can achieve 2.4GB/s (as high as the server’s RAM throughput) for handling reads and 377MB/s for handling writes using a single chip that is not appreciably more expensive than current smart card chips. If more hardware resources are available, the throughput for handling write requests can be increased to 2.4GB/s. Our end-to-end evaluation on file system benchmarks also demonstrates that the prototype system introduces little overhead—around 10% when a client connects to our remote server over the Internet from a corporate network or a fast home network.

8. ACKNOWLEDGEMENTS

We acknowledge the anonymous reviewers for their feedback and the support from Quanta Corporation.

9. REFERENCES

- [1] Amazon. Amazon simple storage service. <http://aws.amazon.com/s3/>.
- [2] Apple. iCloud. <http://www.apple.com/icloud/>.
- [3] P. Bulens, F. Standaert, J. Quisquater, P. Pellegrin, and G. Rouvroy. Implementation of the AES-128 on Virtex-5 FPGAs. *Progress in Cryptology—AFRICACRYPT*, 2008.
- [4] C. Cachin. Integrity and consistency for untrusted services. *SOFSEM 2011: Theory and Practice of Computer Science*, pages 1–14, 2011.
- [5] C. Cachin and M. Geisler. Integrity protection for revision control. In *Applied Cryptography and Network Security*, 2009.
- [6] C. Cachin, I. Keidar, and A. Shraer. Fail-aware untrusted storage. In *IEEE/IFIP International Conference on Dependable Systems & Networks (DSN)*, 2009.

- [7] C. Cachin, A. Shelat, and A. Shraer. Efficient fork-linearizable access to untrusted shared memory. In *Proceedings of the 26th Annual ACM Symposium on Principles of Distributed Computing*, 2007.
- [8] B. Chun, P. Maniatis, S. Shenker, and J. Kubiataowicz. Attested append-only memory: making adversaries stick to their word. In *Proceedings of 21st ACM SIGOPS Symposium on Operating Systems Principles*, 2007.
- [9] V. Costan and S. Devadas. Security challenges and opportunities in adaptive and reconfigurable hardware. In *IEEE International Symposium on Hardware-Oriented Security and Trust (HOST)*, 2011.
- [10] Dropbox. Dropbox. <https://www.dropbox.com/>.
- [11] R. Elbaz, D. Champagne, R. Lee, L. Torres, G. Sassatelli, and P. Guillemin. Tec-tree: A low-cost, parallelizable tree for efficient defense against memory replay attacks. *Cryptographic Hardware and Embedded Systems-CHES*, 2007.
- [12] A. Feldman, W. Zeller, M. Freedman, and E. Felten. SPORC: Group collaboration using untrusted cloud resources. In *Proceedings of the OSDI*, 2010.
- [13] B. Gassend, E. Suh, D. Clarke, M. van Dijk, and S. Devadas. Caches and Merkle trees for efficient memory authentication. In *Proceedings of 9th International Symposium on High Performance Computer Architecture*, 2003.
- [14] S. Ghemawat, H. Gobioff, and S. Leung. The Google file system. In *ACM SIGOPS Operating Systems Review*, 2003.
- [15] E. Goh, H. Shacham, N. Modadugu, and D. Boneh. SiRiUS: Securing remote untrusted storage. In *Proceedings of NDSS*, 2003.
- [16] M. Goodrich, C. Papamanthou, R. Tamassia, and N. Triandopoulos. Athos: Efficient authentication of outsourced file systems. *Information Security*, pages 80–96, 2008.
- [17] Google. Google cloud storage. <https://developers.google.com/storage/>.
- [18] Google. Google drive. <https://drive.google.com/>.
- [19] W. Hall and C. Jutla. Parallelizable authentication trees. In *Selected Areas in Cryptography*, 2006.
- [20] A. Heitzmann, B. Palazzi, C. Papamanthou, and R. Tamassia. Efficient integrity checking of untrusted network storage. In *Proceedings of the 4th ACM International Workshop on Storage Security and Survivability*, 2008.
- [21] M. Kallahalla, E. Riedel, R. Swaminathan, Q. Wang, and K. Fu. Plutus: Scalable secure file sharing on untrusted storage. In *Proceedings of the 2nd USENIX Conference on File and Storage Technologies*, 2003.
- [22] D. Levin, J. Douceur, J. Lorch, and T. Moscibroda. TrInc: small trusted hardware for large distributed systems. In *Proceedings of the 6th USENIX Symposium on Networked Systems Design and Implementation*, 2009.
- [23] J. Li, M. Krohn, D. Mazières, and D. Shasha. Secure untrusted data repository (SUNDR). In *Proceedings of the 6th Conference on Symposium on Operating Systems Design & Implementation*, 2004.
- [24] P. Mahajan, S. Setty, S. Lee, A. Clement, L. Alvisi, M. Dahlin, and M. Walfish. Depot: Cloud storage with minimal trust. In *OSDI, Oct*, 2010.
- [25] D. Mazières and D. Shasha. Don't trust your file server. In *Hot Topics in Operating Systems*, 2001.
- [26] D. Mazières and D. Shasha. Building secure file systems out of Byzantine storage. In *Proceedings of the 21st Annual ACM Symposium on Principles of Distributed Computing*, 2002.
- [27] R. Merkle. Protocols for public key cryptosystems. In *IEEE Symposium on Security and Privacy*, 1980.
- [28] J. Ousterhout. Why aren't operating systems getting faster as fast as hardware? Technical report, Digital Equipment Corporation Westem Research Laboratory, Oct. 1989.
- [29] R. Popa, J. Lorch, D. Molnar, H. Wang, and L. Zhuang. Enabling security in cloud storage SLAs with CloudProof. Technical report, Microsoft, 2010.
- [30] W. Rankl and W. Effing. *Smart card handbook*. Wiley, 2010.
- [31] R. Sandberg, D. Goldberg, S. Kleiman, D. Walsh, and B. Lyon. Design and implementation of the Sun network filesystem. In *Proceedings of the Summer USENIX conference*, 1985.
- [32] S. Shepler, B. Callaghan, D. Robinson, R. Thurlow, C. Beame, M. Eisler, and D. Noveck. Network file system (NFS) version 4 protocol. RFC 3530, Network Working Group, Apr. 2003.
- [33] A. Shraer, C. Cachin, A. Cidon, I. Keidar, Y. Michalevsky, and D. Shaket. Venus: Verification for untrusted cloud storage. In *Proceedings of the 2010 ACM Workshop on Cloud Computing Security*, 2010.
- [34] N. Sklavos, E. Alexopoulos, and O. Koufopavlou. Networking data integrity: High speed architectures and hardware implementations. *Int. Arab J. Inf. Technol*, 1:54–59, 2003.
- [35] Trusted Computing Group. Trusted Platform Module (TPM) Specifications. <https://www.trustedcomputinggroup.org/specs/TPM/>.
- [36] M. van Dijk, J. Rhodes, L. Sarmenta, and S. Devadas. Offline untrusted storage with immediate detection of forking and replay attacks. In *Proceedings of the 2007 ACM Workshop on Scalable Trusted Computing*, 2007.
- [37] H.-J. Yang. Efficient trusted cloud storage using parallel, pipelined hardware. Master's thesis, Massachusetts Institute of Technology, 2012.